# Modeling and Nonlinear Adaptive Control for Autonomous Vehicle Overtaking

Plamen Petrov and Fawzi Nashashibi, *Member, IEEE*

***Abstract*—In this paper, we present a mathematical model and adaptive controller for an autonomous vehicle overtaking maneuver. We consider the problem of an autonomous three-phase overtaking without the use of any roadway marking scheme or intervehicle communication. The developed feedback controller requires information for the current relative intervehicle position and orientation, which are assumed to be available from onboard sensors. We apply standard robotic nomenclature for translational and rotational displacements and velocities and propose a general kinematic model of the vehicles and the relative intervehicle kinematics during the overtaking maneuver. The overtaking maneuver is investigated as a tracking problem with respect to desired polynomial virtual trajectories for every phase, which are generated in real time. An update control law for the automated overtaking vehicle is designed that allows tracking the desired trajectories in the presence of unknown velocity of the overtaken vehicle. Simulation results illustrate the performance of the proposed controller.**

***Index Terms*—Adaptive control, autonomous vehicles, intelligent transportation system, lateral and longitudinal control.**

## I. Introduction

In RECENT years, there have been significant interest and research activity in the area of cooperative control of multiple automated vehicles. The ultimate goal in automating the driving process is to reduce accidents caused by human error and improve safety. At the same time, the full automation can greatly increase the roadway capacity and diminish air pollution by efficient use of fuel. Fully automated vehicle operation is realized through different kinds of maneuvers such as lane following, lane changing, merging, splitting, platooning, and overtaking, which have been extensively studied and also experimentally demonstrated during the last decades. In 1997, California's Partners for Advanced Transit Highways (PATH) team demonstrated at DEMO'97 [1], eight PATH vehicles under fully automated control performing functions, including platooning, lane keeping, lane change, and platoon split and merge maneuvers. Recently, the automatic vehicle following capabilities for passenger vehicles [2]–[5] and trucks [6] have been demonstrated during the Grand Cooperative Driving Challenge 2011 (GCDC 2011), in Netherlands. The benefits are well understood, platooning demonstrations have established credibility and technical feasibility of implementing such a technique in the existing roads. In addition, a series of EU-funded projects, such as Cybercars and CyberCars 2 [7], HAVEit [8], and ECOVISION [9], were addressed the issue of automated driving such as adaptive cruise control, lane keeping, lane change, stop & go, and platooning. The main objective of these projects was to accelerate the development and implementation of cybernetic transportation systems for people and goods in urban environments.

A major long-term element of research and development of automated vehicles is vehicle control. The control strategies required for this purpose depend on the information available for each vehicle controller. The intervehicle communication, particularly concerning vehicle position, orientation, velocity (and eventually acceleration), largely simplifies the control scheme of an automated vehicle. The autonomous vehicle operation (without intervehicle communication) in different maneuvers of automated vehicles has also attracted attention in the last decades [10]. Using onboard sensors such as laser scanning radar units [11] and cameras [8], [9], some quantities as intervehicle position and orientation can be measured, and other quantities as relative velocity and acceleration/deceleration can be estimated from the measured quantities [12]. In this case, high-gain observers or adaptive control (as in [12]) can be used to replace direct measurements and intervehicle communications of some quantities required in the feedback control scheme of the automated car.

The automated vehicle overtaking is one of the most complex maneuvers for road automation. In contrast to lane-keeping and lane-change maneuvers, the overtaking is a composition of three consecutive maneuvers, namely, lane change followed by traveling a specified path parallel to the overtaken vehicle in an adjacent line (lane keeping), and again, a lane change, which have to be planned and coordinated. The lane-keeping system deals with the control of the steering movement in order to keep the automated vehicle to travel along a prescribed path. Often, the automatic control of the longitudinal and lateral motion of the vehicle is separately undertaken, and each controller is designed as if the longitudinal and steering vehicle dynamics is decoupled [13]. Different lateral controllers have been proposed, such as a linear time-invariant lane-keeping controller, based on the bicycle model was presented in [14], an adaptive lane-keeping controller was proposed in [15] In order to deal with the vehicle dynamics uncertainty and parameter variation, robust (sliding mode [16]) and adaptive [17] lane-keeping controllers were proposed. A combined longitudinal and lateral controller, which achieves asymptotically stable

Manuscript received February 17, 2013; revised June 14, 2013 and November 28, 2013; accepted January 18, 2014. Date of publication March 3, 2014; date of current version August 1, 2014. This work was supported by the ABV project. The Associate Editor for this paper was S. A. Wadoo.

P. Petrov is with the Faculty of Mechanical Engineering, Technical University of Sofia, 4000 Sofia, Bulgaria (e-mail: ppetrov@ tu-sofia.bg).

F. Nashashibi is with the Institut National de la Recherche en Informatique et Automatique (INRIA), 78153 Rocquencourt, France (e-mail: Fawzi.Nashashibi@inria.fr).

Color versions of one or more of the figures in this paper are available online at http://ieeexplore.ieee.org.

Digital Object Identifier 10.1109/TITS.2014.2303995

trajectory without measurement of the lateral vehicle velocity and accurate knowledge of the vehicle parameters were reported in [18]. The objective of the lane-change maneuver is to transfer a vehicle that is is under lane following control to lane following in an adjacent lane [19]. During the lane-change maneuver, the vehicle should have predefined (desired) trajectory to track. The existing desired trajectories can be categorized based on the types of curves that generate, namely, circular [20], harmonic [21], spline [22], and polynomial [23], [24] line segments, which, in general, should be functions of time. Nonlinear control techniques as sliding mode [25] and robust switching control [26] have been used for designing lane-change controllers.

Compared with lane keeping and lane changing, overtaking is even more challenging problem, because it is a composition of consecutive maneuvers (lane change, followed by lane tracking, and again—lane change), which have to be coordinated. In the automated vehicle overtaking, the control objective can be realized using infrastructure-supported approach or in autonomous fashion. The infrastructure-supported approach is based on trajectories, which can be physically or virtually marked, and often, in combination with intervehicle communication. In this case, the system is not completely interconnected, since during the second phase (lane keeping) of the overtaking maneuver, each vehicle independently follows proper reference lane. In the autonomous overtaking approach, only onboard sensors are used to determine the relative position and orientation between vehicles without any roadway marking scheme or intervehicle communication. The steering commands for the controlled vehicle are set according to the relative position and orientation with respect to the overtaken car and, in that way, the overtaking vehicle accomplishes the maneuver with respect to the overtaken vehicle instead of the road [27]. While considerable research work has been reported on lane-keeping and lane-change maneuver, the problem of automated overtaking has attracted less attention. In [28], an optimal trajectory for an overtaking maneuver was designed by formulating a nonlinear constrained optimization problem. The solution of the optimization problem determines the optimal time and distance for the lane-change maneuver using fifth-degree polynomial functions. An online time-optimal trajectory planning algorithm for the guidance of a pursuer vehicle overtaking a slower vehicle, which is based on the Rendezvous-Guidance principle was proposed in [29]. A planning algorithm using lateral potentials for autonomous vehicles in the absence of speed lanes was proposed in [30]. A two-layer controller architecture for overtaking maneuver is presented in [31]. The lower level consists of two fuzzy steering controllers for path tracking and lane change, and the high level is to evaluate the necessity and possibility of overtaking, and to switch between the low-level controllers. The route tracking system is based on the information supplied by the GPS, which digitally maps the driving zone for circulation and the vehicles know their positions on the road using wireless communication (in the framework of Autopia program). An overtaking control method based on the estimation of the conflict probability as safe indicator was proposed in [32]. The method uses model predictive control and integrates decision making and control of the overtaking maneuver into a tracking control problem. An on-road demonstration of cooperative driving solutions and, in particular, overtaking maneuver by autonomous road vehicles designed for the cities is reported in [33]. An automatic overtaking system is presented in [34]. A fuzzy logic-based controller was developed to this, which was based on information obtained from vision system, differential global position system (DGPS) and inertial measurement unit. The system has been incorporated into a commercial car and successfully tested with different preceding vehicles—motorbike, car, and truck.

In this paper, we propose a mathematical model and nonlinear adaptive controller for a two-vehicle automated overtaking maneuver. We consider the problem of autonomous overtaking without the use of road infrastructure with only the current intervehicle position and orientation available for feedback control, which is assumed to be available from onboard sensors such as laser range finders and cameras. A preliminary version of this paper was presented at the 2011 International IEEE Conference on Intelligent Transportation Systems [27]. Compared with our previous work, in this paper, by applying standard robotic nomenclature for translational and rotational displacements and velocities, we develop a methodology for kinematic modeling of the vehicles and propose a general kinematic model of the relative intervehicle kinematics during the overtaking maneuver. We also describe a possible extension in case of multivehicle overtaking. We enlarge our previous work and consider the case of time-varying velocity of the overtaken vehicle during the maneuver. We present a stability analysis of the closed-loop control system in case of bounded variation of the velocity of the overtaken vehicle, which is also validated by new simulation results for different scenarios. Our approach for the overtaking maneuver consists in consecutive tracking of reference virtual points, which are positioned at desired *a priori* known distances from the overtaken vehicle with a virtual reference point attached to the overtaking vehicle. The reference trajectories for the desired motion of the overtaking vehicle during the overtaking maneuver are generated using polynomial functions. The overtaking maneuver is considered as a tracking problem. An adaptive nonlinear controller for the overtaking vehicle is designed that allows tracking desired trajectories in the presence of unknown velocity of the overtaken vehicle. The use of an adaptive control strategy is motivated from the need of estimating the velocity of the overtaking vehicle, which is necessary for feedback control under autonomous vehicle operation (without intervehicle communication). The stability of the closed-loop system is analytically studied and asymptotic stability of the closed-loop control system is proved in case of constant velocity of the overtaken vehicle. In addition, in case of time varying but bounded velocity, ultimate boundness of the system tracking error is claimed. Simulation results are presented, in order to illustrate the performance of the propose controller. The organization of this paper is as follows: In Section II, the mathematical description of a three-phase overtaking maneuver suitable for feedback control is derived. The problem formulation is given in Section III. In Section IV, a nonlinear adaptive control law is designed and stability analysis is performed. Section V contains simulation results. Conclusions are presented in Section VI.

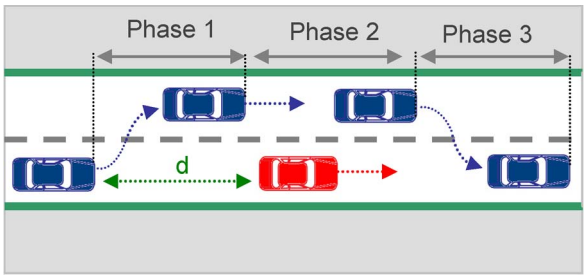


Fig. 1. Three-phase overtaking maneuver involving two vehicles.

## II. Mathematic Model

### A. Three-Phase Overtaking Maneuver

In this paper, the overtaking involving two vehicles is established as a three-phase maneuver, illustrated in Fig. 1. During the overtaking maneuver, we assume that the following conditions are met:

- The overtaken vehicle is moving along a rectilinear route.
- The linear velocity of the overtaken vehicle is unknown.
- The available information for feedback control is the relative intervehicle position and orientation.

A brief description of the three-phase overtaking scenario considered in this paper is provided below. Assume that the automated vehicle has to pass the preceding car, which is at distance $d$ ahead. The first phase consists of a "lane-change"-type maneuver. Starting with some initial conditions, the overtaking vehicle diverts from the lane and tracks a given reference trajectory for a given time period and has to reach a preselected position behind the overtaken vehicle (see Fig. 1). At the end of the first time period, which is determined by the time duration (transition time) assigned for the desired trajectory for Phase 1 (denoted by $t_f$ in Section III-A), the guidance program switches from Phase 1 to Phase 2. The second phase consists of driving along the overtaken vehicle at a prescribed lateral distance. The vehicle tracks again a given reference trajectory for a prescribed time period until the overtaken vehicle has been passed, and the overtaking vehicle reaches a preselected position on the left side of the overtaken vehicle. During the third phase, given a reference trajectory for the third phase, the overtaking vehicle returns to the lane and has to reach a preselected position in front of the overtaken vehicle. A reference trajectory for the overtaking vehicle is generated in real time for every phase. The desired position and linear velocity of the overtaking vehicle with respect to the overtaken vehicle at the end of every phase, as well as the phase duration, are determined to satisfy the operational requirements imposed on such a maneuver. A specific feature of the proposed trajectory planning procedure is that at the beginning of each phase, the desired initial position and velocity of the overtaking vehicle coincides with its current position and velocity. In such way, a smooth transition between the adjacent phases is assured. Furthermore, trajectory tracking controller has to regulate to zero small tracking errors during the predetermined time associated with each phase of the overtaking maneuver.

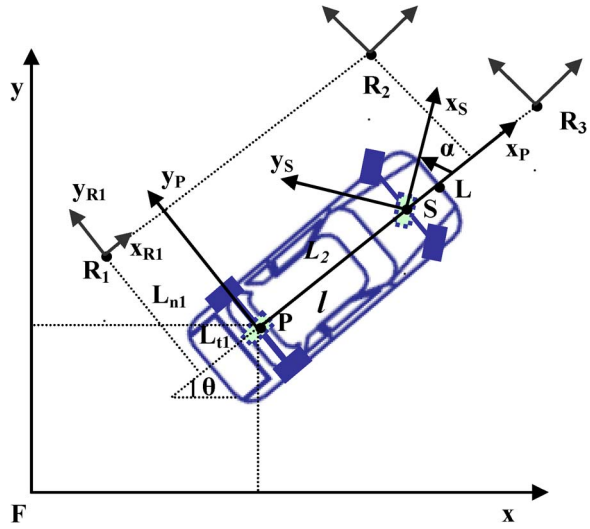


Fig. 2. Vehicle coordinate frame assignment.

### B. Vehicle Kinematics

*1) Coordinate System Assignments:* In order to model the kinematics of the vehicles during the overtaking maneuver, we apply standard robotic nomenclature for translational and rotational displacements and velocities, and methodology [35]. It is assumed that the wheels roll without sliding, and the slip angles of the wheels are negligible. In this case, the velocity vectors of the wheels are in the direction of the orientation of the wheels, and classical methods from analytic mechanics can be used to develop mathematical models of the vehicle as a nonholonomic system. Fig. 2 depicts the schematic of the vehicles considered in this paper. To simplify the derivation of the vehicle control algorithms, we use a planar bicycle 2DOFs vehicle model where two virtual wheels are located at the midpoints of the front and rear wheel axles (see Fig. 2). Although these two wheels do not exist, it is assumed that they comply with the condition of wheel rolling without slipping.

In order to describe the position and orientation of the vehicles in the plane during the overtaking maneuver, we assign the following coordinate frames (see Fig. 2):

- $Fxy$—inertial coordinate frame in the plane of motion;
- $Px_Py_P$—vehicle coordinate frame located at the center of the rear vehicle axis, where the $x$-axis is along the longitudinal base of the vehicle. The coordinates of a reference point $P$ placed at the center of the rear vehicle axle, with respect to $Fxy$, are denoted by $(x_P, y_P)$.
- $R_1x_{R1}y_{R1}$, $R_2x_{R2}y_{R2}$, $R_3x_{R3}y_{R3}$—moving virtual reference frames rigidly attached to the overtaken vehicle, which centers are located at prescribed distances $(L_{t1}, L_{n1})$, $(L_{t2}, L_{n2})$, and $(L_{t3}, L_{n3})$, respectively, from the coordinate system $Px_Py_P$ attached to the overtaken vehicle. The $x_R$- and $y_R$-axis of these coordinate systems are parallel to the corresponding $x_P$- and $y_P$-axis of the frame $PxPy$.
- $Lx_Ly_L$—coordinate frame rigidly linked to the overtaking vehicle and located at the midpoint of the front bumper of the vehicle at a distance $L_2$ from point $P$,

where the $x_L$-axis is in the direction of the longitudinal vehicle axle.

— $Sx_Sy_S$—wheel coordinate system with origin placed at the center of the virtual front steering wheel; the $x_s$-axis is in the direction of the wheel orientation.

The assignment of the moving virtual coordinate systems $R_1x_{R1}y_{R1}$, $R_2x_{R2}y_{R2}$, and $R_3x_{R3}y_{R3}$ attached to the overtaken vehicle are related to the places and orientation that the overtaking vehicle has to reach at the end of each phase of the three-phase overtaking maneuver. The underlying idea behind this is to introduce virtual points, which are assigned to lie on the desired path of the overtaking vehicle and are used as consecutive "targets" for its trajectory. The prescribed distances $(L_{t1}, L_{n1})$, $(L_{t2}, L_{n2})$, and $(L_{t3}, L_{n3})$ are basically determined from considerations of safety driving and vehicle geometrical limitations (for example, $L_{n1}$ must be grater than the sum of the half-widths of the overtaken and overtaking vehicle).

The longitudinal base $PS$ of the vehicle is denoted by $l$. Angle $\theta$ is the orientation angle of the vehicle with respect to frame $Fxy$. The front-wheel steering angle $\alpha$ is measured with respect to the longitudinal vehicle axis $x_P$. We note here that subscript indexes "1" and "2" will be added to the notations introduced above when it is necessary to refer to a particular vehicle, i.e., the overtaken and overtaking vehicle, respectively. For example, $\theta_1$ will denote the orientation angle of the overtaken vehicle, and $\theta_2$ will denote the orientation angle of the overtaking vehicle; $P_1x_{P1}y_{P1}$ will denote vehicle coordinate frame located at the center of the rear axis of the overtaken vehicle. However, for clarity of exposition, when it is possible, the subscript index will be often omitted when deriving expressions for the vehicle equations of motion, and these expressions take the same form irrespective of whether they correspond to the overtaken or the overtaking vehicle and are evident from the context. Since the vehicle is assumed to move on a planar surface, in what follows, we use $3 \times 3$ rather than $4 \times 4$ homogeneous transformation matrices ${}^{A}T_{B}$ to transform the coordinates of a point $G$ from coordinate system $B$ denoted by ${}^{B}p_G$ to its corresponding coordinates ${}^{A}p_G$ in the coordinate frame $A$. Again, the subscript indexes will be added to refer to point coordinates and transformation matrices associated with a particular vehicle. For example, the transformation matrix ${}^{F}T_{P_2}$ defines the position and orientation of coordinate system $P_2x_{P2}y_{P2}$ located at the center of the rear vehicle axis of the overtaking vehicle relative to inertial coordinate frame $F$.

Using the above notations, the assignment of the coordinate frames results in the following transformation matrices between the coordinate systems:

$$ {}^{P}T_S = \begin{bmatrix} \cos\alpha & -\sin\alpha & l \\ \sin\alpha & \cos\alpha & 0 \\ 0 & 0 & 1 \end{bmatrix} \tag{1} $$

$$ {}^{F}T_P = \begin{bmatrix} \cos\theta & -\sin\theta & {}^{F}x_P \\ \sin\theta & \cos\theta & {}^{F}y_P \\ 0 & 0 & 1 \end{bmatrix}. \tag{2} $$

The transformation matrices (1) and (2) are applied to determine the position kinematics of the vehicle.

Using (1) and (2), the position of point $S$ in the inertial frame $F$ is

$$ \begin{aligned} {}^{F}p_S &= {}^{F}T_P\,{}^{P}T_S\,{}^{S}p_S \\ &= \begin{bmatrix} \cos\theta & -\sin\theta & {}^{F}x_A \\ \sin\theta & \cos\theta & {}^{F}y_A \\ 0 & 0 & 1 \end{bmatrix} \begin{bmatrix} \cos\alpha & -\sin\alpha & l \\ \sin\alpha & \cos\alpha & 0 \\ 0 & 0 & 1 \end{bmatrix} \begin{bmatrix} 0 \\ 0 \\ 1 \end{bmatrix} \\ &= \begin{bmatrix} x_P + l\cos\theta \\ y_P + l\sin\theta \\ 1 \end{bmatrix}. \end{aligned} \tag{3} $$

The homogeneous coordinates of each reference point $R$ associated with the overtaken vehicle in frame $Fxy$ are determined by using (2) as

$$ {}^{F}p_R = {}^{F}T_P\,{}^{P}p_R \tag{4} $$

where

$$ {}^{P}p_R = [L_t \quad L_n \quad 1]^T. \tag{5} $$

Similarly, the homogeneous coordinates of the front reference point $L$ associated with the overtaking vehicle in frame $Fxy$ are

$$ {}^{F}p_L = {}^{F}T_{P_2}\,{}^{P_2}p_L \tag{6} $$

where

$$ {}^{P_2}p_L = [L_2 \quad 0 \quad 1]^T. \tag{7} $$

*2) Nonholonomic Constraints:* If the rotation of the wheels with respect to their proper axes is ignored, the vehicle configuration can be described by four generalized coordinates, i.e.,

$$ q_i = \left[{}^{F}x_P, {}^{F}y_P, \theta, \alpha\right]^T \in \Re^4. \tag{8} $$

Differentiating (3), the components of the velocity of point $S$ with respect to the inertial frame $Fxy$ and expressed in the $Fxy$ frame are

$$ {}^{F}\dot{p}_S = \begin{bmatrix} {}^{F}\dot{x}_S \\ {}^{F}\dot{y}_S \\ 0 \end{bmatrix} = \begin{bmatrix} {}^{F}\dot{x}_P - l\dot{\theta}\sin\theta \\ {}^{F}\dot{y}_P + l\dot{\theta}\cos\theta \\ 0 \end{bmatrix}. \tag{9} $$

In order to derive the nonholonomic constraints of the front virtual wheel, the components of the velocity of point $S$ relative to frame $Fxy$ are expressed in frame $Sx_Sy_S$ as follows:

$$ \begin{aligned} {}^{S}\dot{p}_S &= \begin{bmatrix} {}^{S}v_{Sx} \\ {}^{S}v_{Sy} \\ 0 \end{bmatrix} = \left({}^{F}T_P\,{}^{A}T_S\right)^{-1}\,{}^{F}\dot{p}_S \\ &= \begin{bmatrix} \cos(\theta+\alpha) & \sin(\theta+\alpha) & * \\ -\sin(\theta+\alpha) & \cos(\theta+\alpha) & * \\ 0 & 0 & 1 \end{bmatrix} \begin{bmatrix} {}^{F}\dot{x}_S \\ {}^{F}\dot{y}_S \\ 0 \end{bmatrix} \end{aligned} \tag{10} $$

where the terms indicated by $(*)$ are irrelevant in the computation. Based on the assumption of rolling without lateral sliding, we have ${}^{S}v_{Sy} = 0$, where ${}^{S}v_{Sy}$ is the component of the velocity of point $S$ along the $y$-axis of frame $Sx_Sy_S$. From the second

line of equality (10) and by using expressions (9) for ${}^F\dot{p}_S$, the nonholonomic constraint for the front virtual wheel can be written in the form, i.e.,

$$0 = -{}^F\dot{x}_P \sin(\theta+\alpha) + {}^F\dot{y}_P \cos(\theta+\alpha) + l\dot{\theta}\cos\alpha. \quad (11)$$

Likewise, using (2), the nonholonomic constraint imposed on the rear virtual wheel (${}^P v_{Py} = 0$) can be derived from the second line of the following expression:

$$\begin{aligned} {}^P\dot{p}_P &= \begin{bmatrix} {}^P v_{Px} \\ {}^P v_{Py} \\ 0 \end{bmatrix} = {}^F T_P^{-1\,F}\dot{p}_P \\ &= \begin{bmatrix} \cos\theta & \sin\theta & * \\ -\sin\theta & \cos\theta & * \\ 0 & 0 & 1 \end{bmatrix} \begin{bmatrix} {}^F\dot{x}_P \\ {}^F\dot{y}_P \\ 0 \end{bmatrix} \end{aligned} \quad (12)$$

in the form

$$0 = -{}^F\dot{x}_P \sin\theta + {}^F\dot{y}_P \cos\theta. \quad (13)$$

Combining (11) and (13), the vehicle nonholonomic constraints can be written in matrix form as

$$C_a(q)\dot{q} = 0 \quad (14)$$

where

$$C_a(q) = \begin{bmatrix} -\sin\theta & \cos\theta & 0 & 0 \\ -\sin(\theta+\alpha) & \cos(\theta+\alpha) & l\cos\alpha & 0 \end{bmatrix} \quad (15)$$

is a $2 \times 4$ full rank matrix and

$$\dot{q} = [\, {}^F\dot{x}_P \quad {}^F\dot{y}_P \quad \dot{\theta} \quad \dot{\alpha}\,]^T \quad (16)$$

is the vector of generalized velocities. The number of degrees of freedom (DOF) of the vehicle is 2 and is equal to the difference between the number of the generalized coordinates (8) and the noholonomic constraints (14) [36]. Let us introduce linear forms of the generalized velocities (the so-called quasi-velocities), which are equal to the left side of (14) as follows:

$$\eta_a = \begin{bmatrix} {}^S v_{Sy} \\ {}^P v_{Py} \end{bmatrix} = C_A(q)\dot{q}. \quad (17)$$

Hence, the nonholonomic constraints (14) can be written in the form

$$\eta_a = 0. \quad (18)$$

In the same way, we introduce nonzero quasi-velocities, which number is equal to the number of DOF of the system as follows:

$$\eta_b = \begin{bmatrix} {}^P v_{Px} \\ \omega_\alpha \end{bmatrix} = C_B(q)\dot{q} \quad (19)$$

where ${}^P v_{Px}$ is the component of the velocity of point $P$ along the $x$-axis of frame $Px_Py_P$, $\omega_\alpha$ is the steering angular velocity of the front virtual wheel, and the $2 \times 4$ matrix $C_B$ is given by

$$C_b(q) = \begin{bmatrix} \cos\theta & \sin\theta & 0 & 0 \\ 0 & 0 & 0 & 1 \end{bmatrix}. \quad (20)$$

Using (17) and (19), the quasi-velocities $\eta = [\eta_a \,|\, \eta_b]^T \in R^4$ can be expressed in the form

$$\eta = C(q)\dot{q} \quad (21)$$

where the $4 \times 4$ block-matrix $C$ has the form

$$C(q) = \begin{bmatrix} C_a(q) \\ -- \\ C_b(q) \end{bmatrix}. \quad (22)$$

If $\det C \neq 0$, (21) can be solved with respect to the generalized velocities $\dot{q}$

$$\dot{q} = C^{-1}(q)\eta \quad (23)$$

where the matrix $C^{-1}(q) := D(q)$ has the form

$$\begin{aligned} C^{-1}(q) := D(q) &= [D_a(q)|D_b(q)] \\ &= \left[\begin{array}{cc|cc} 0 & -\sin\theta & \cos\theta & 0 \\ 0 & \cos\theta & \sin\theta & 0 \\ \frac{1}{l\cos\alpha} & \frac{1}{l} & \frac{\sin\alpha}{l\cos\alpha} & 0 \\ 0 & 0 & 0 & 1 \end{array}\right]. \end{aligned} \quad (24)$$

Using (18), (23) takes the form of an affine driftless control system

$$\dot{q} = D_b(q)\eta_b \quad (25)$$

where the columns of the $4 \times 2$ matrix $D_b(q)$

$$D_b(q) = \begin{bmatrix} \cos\theta & 0 \\ \sin\theta & 0 \\ \frac{\tan\alpha}{l} & 0 \\ 0 & 1 \end{bmatrix} \quad (26)$$

are in the null space of $C_a(q)$, i.e., $C_a(q)D_b(q) = 0$.

In the following, we consider the vehicle angular velocity (the front-wheel steering angle $\alpha_2$, respectively) as a control input instead of the steering angle velocity. From the third equation of (26), the front-wheel steering angle can be expressed in terms of the vehicle angular velocity as follows:

$$\alpha = a\tan\left(l\frac{\dot{\theta}}{{}^P v_{Px}}\right). \quad (27)$$

Let us denote by

$${}^F z_R = [\, {}^F x_R \quad {}^F y_R \quad \theta_1\,]^T \in \Re^3 \quad (28)$$

the pose of the overtaken vehicle in the inertial frame $Fxy$ expressed in terms of the coordinates of reference point $R$. Differentiating (4) and using the first two equations of (26), a kinematic model of the overtaken vehicle based on each reference point $R$, can be written in the form

$${}^F\dot{z}_R = A_1\eta_{e1} \quad (29)$$

where

$$A_1 = \begin{bmatrix} \cos\theta_1 & 0 & -L_t\sin\theta_1 + L_n\cos\theta_1 \\ \sin\theta_1 & 0 & L_t\cos\theta_1 - L_n\sin\theta_1 \\ 0 & 0 & 1 \end{bmatrix} \quad (30)$$

$$\eta_{e1} = [\, {}^{P_1} v_{P_1 x} \quad 0 \quad \omega_1\,]^T \quad (31)$$

and $\omega_1 := \dot{\theta}_1$ is the angular velocity of the overtaken vehicle.

*Remark 1:* Here, the derivation of the overtaken vehicle kinematic model has been oriented to left-side overtaking, which is the basic case of overtaking. However, the procedure of deriving a kinematic model of the overtaken vehicle based on the reference points $R_1$, $R_2$, and $R_3$ can be also applied in the case of right-side overtaking by assigning reference points $R_1$ and $R_2$ in the reciprocal position of the points for left-side overtaking shown in Fig. 2. In this case, the vector (5), which describes the coordinates of the reference points $R$ in the coordinate frame located at the center of the rear vehicle axis of the overtaken vehicle takes the form ${}^{P}p_R = [L_t \quad -L_n \quad 1]^T$. Due to the limited space, we omit further details of the derivation of the overtaken vehicle kinematic model for right overtaking, which has a slightly different expression from those, obtained in (30) for left-side overtaking.

Similarly, let us denote by

$$ {}^{F}z_L = [\,{}^{F}x_L \quad {}^{F}y_L \quad \theta_2\,]^T \in \Re^3 \tag{32}$$

the pose of the overtaking vehicle in the inertial frame $Fxy$ expressed in terms of the coordinates of reference point $L$. Differentiating (6) and using the first two equations of (26), a kinematic model of the overtaking vehicle based on the reference point $L$ is obtained as follows:

$$ {}^{F}\dot{z}_L = A_2 \eta_{e2} \tag{33}$$

where

$$ A_2 = \begin{bmatrix} \cos\theta_2 & 0 & L_2 \sin\theta_2 \\ \sin\theta_2 & 0 & L_2 \cos\theta_2 \\ 0 & 0 & 1 \end{bmatrix} \tag{34}$$

$$ \eta_{e2} = [\,{}^{P_2}v_{P_2x} \quad 0 \quad \omega_2\,]^T \tag{35}$$

and $\omega_2 := \dot{\theta}_2$ is the angular velocity of the overtaking vehicle.

### C. Relative Kinematics

A schematic plan view of an overtaking maneuver involving two vehicles is shown in Fig. 3. The three coordinate frames $R_1x_{R1}y_{R1}$, $R_2x_{R2}y_{R2}$, $R_3x_{R3}y_{R3}$, and $Lx_Ly_L$ are defined to describe the relative intervehicle kinematics during each of the three phases of the overtaking maneuver. For this purpose, we define a error pose (the coordinates and orientation of the frame $Lx_Ly_L$ in the coordinate frame $Rx_Ry_R$), by the vector

$$ e = [\,e_x \quad e_y \quad e_\theta\,]^T \in \Re^3. \tag{36}$$

Using (28) and (32), the error pose vector can be expressed as follows [37]:

$$ e = R\left({}^{F}z_L - {}^{F}z_R\right) \tag{37}$$

where

$$ R = \begin{bmatrix} \cos\theta_1 & \sin\theta_1 & 0 \\ -\sin\theta_1 & \cos\theta_1 & 0 \\ 0 & 0 & 1 \end{bmatrix}. $$

Differentiating (37) with respect to time and taking into account equations (29) and (33), after some work, the intervehicle kinematics in error coordinates is obtained as follows:

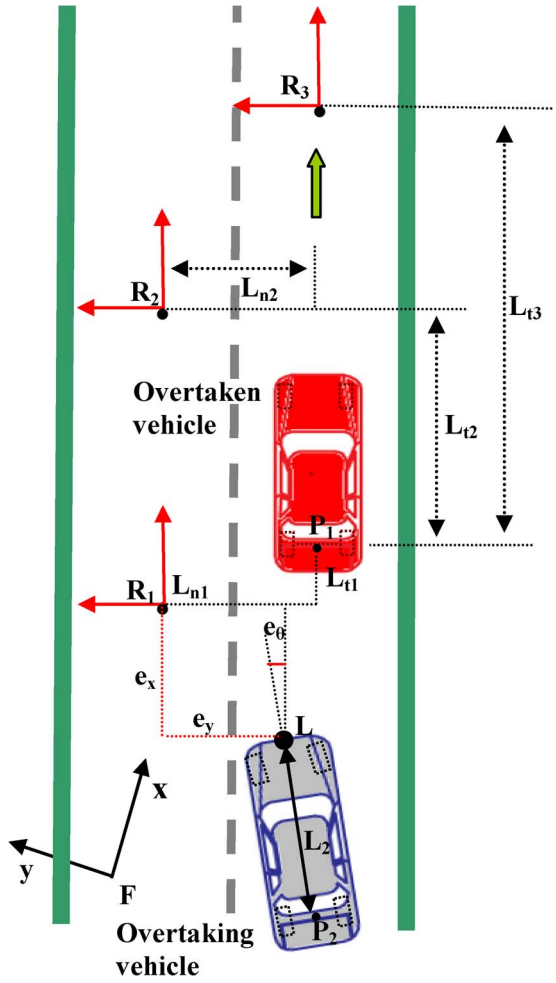


Fig. 3. Schematics of the overtaking maneuver.

$$ \begin{bmatrix} \dot{e}_x \\ \dot{e}_y \\ \dot{e}_\theta \end{bmatrix} = \begin{bmatrix} \cos e_\theta & 0 & -L_2 \sin e_\theta \\ \sin e_\theta & 0 & L_2 \cos e_\theta \\ 0 & 0 & 1 \end{bmatrix} \begin{bmatrix} v_{2x} \\ 0 \\ \omega_2 \end{bmatrix} - \begin{bmatrix} 1 & 0 & -L_n \\ 0 & 0 & -L_t \\ 0 & 0 & 1 \end{bmatrix} \begin{bmatrix} v_{1x} \\ 0 \\ \omega_1 \end{bmatrix} + \omega_1 \begin{bmatrix} 0 & 1 & 0 \\ -1 & 0 & 0 \\ 0 & 0 & 0 \end{bmatrix} \begin{bmatrix} e_x \\ e_y \\ e_\theta \end{bmatrix} \tag{38}$$

where $v_{1x} := {}^{P_1}v_{P_1x}$ and $v_{2x} := {}^{P_2}v_{P_2x}$ are the longitudinal components of the linear velocities of points $P_1$ and $P_2$, respectively, associated with the overtaken and overtaking vehicle, respectively.

Based on the assumption of pure rolling without a lateral sliding of the wheels, the nonholonomic constraints imply that in (38), the components of the velocities of points $P_1$ and $P_2$ in the direction of the rear vehicle axles are equal to zero, i.e., $v_{1y} := {}^{P_1}v_{P_1y} = 0$ $v_{2y} := {}^{P_2}v_{P_2y} = 0$. This is due to the fact that velocity vectors of the wheels are in the direction of the wheels, and the rear wheels are parallel to the longitudinal vehicle axle (the center of the wheels and midpoint $P$ are situated on the rear vehicle axle, which is perpendicular to the $x_P$-axis of coordinate frame $Px_Py_P$). Notice that (38) describes the relative kinematics of the vehicles in the general case for curvilinear motion of the vehicles.

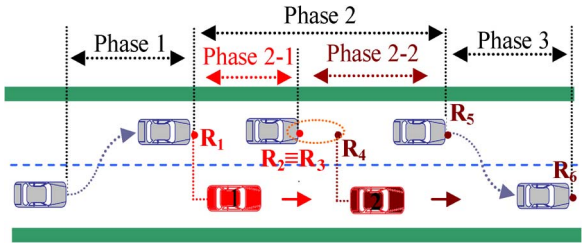


Fig. 4. Schematics of the multivehicle overtaking maneuver.

In the following, we consider an overtaking maneuver during rectilinear motion of the overtaken vehicle. In this case, the angular velocity of the overtaking vehicle $\omega_1 = 0$.

Let us consider the following change of inputs in (38):

$$\begin{bmatrix} u_1 \\ u_2 \end{bmatrix} = \begin{bmatrix} \cos e_\theta & -L_2 \sin e_\theta \\ \sin e_\theta & L_2 \cos e_\theta \end{bmatrix} \begin{bmatrix} v_{2x} \\ \omega_2 \end{bmatrix} \tag{39}$$

where it can be easily verified that the transformation matrix is nonsingular when $L_2 \neq 0$. Using (39), in case of rectilinear motion of the overtaken vehicle, the intervehicle kinematic equations (4) can be written in the form

$$\begin{aligned} \dot{e}_x &= u_1 - v_{2x} \\ \dot{e}_y &= u_2 \\ \dot{e}_\theta &= -\frac{\sin e_\theta}{L_2} u_1 + \frac{\cos e_\theta}{L_2} u_2. \end{aligned} \tag{40}$$

*Remark 2:* The methodology for modeling one-vehicle overtaking proposed here can be easily extended to multivehicle overtaking. The multiple overtaking again could be considered as a three-phase maneuver, but the second phase will be broadly divided into subphases, which number is equal to the number of the overtaken vehicles. We note again that the reference points $R_1$, $R_2$, and $R_3$ attached to the overtaken vehicle (see Fig. 3) are assigned to lie on the desired path of the overtaking vehicle and are used as *consecutive* targets for its trajectory (see Section III-A). In Fig. 4, we depict a typical two-vehicle overtaking in order to introduce the coordinate system assignment in case of multiple overtaking. Since the overtaking maneuver requires a combination of decision and control actions, once the decision for overtaking vehicle 2 has been taken in order to "intercept" overtaken vehicle 2, instead of going in front of overtaken vehicle 1, the overtaking vehicle has to skip the third phase of the one-vehicle overtaking maneuver. At this end, we leave the freedom for assigning $R_3$ at positions that lead to a convenient form of the kinematic model of the overtaken vehicle 1, depending on whether one- or two-vehicle overtaking needs to be carried out. By keeping the three-point model, in addition to the previous assigned place for $R_1$ in front of vehicle 1, we introduce also the possibility to arrange point $R_3$ to coincide with point $R_2$. We formalize this by setting $L_{t3} = L_{t2}$ and $L_{n3} = L_{n2}$ for the third phase. This superposition of coordinate frames eliminates the subsequent derivation of the kinematic model of the overtaken vehicle, the corresponding relative kinematics, and the trajectory planning for this phase. Using this approach, the position and orientation of the overtaking vehicle with respect to vehicle 1 at $R_2 \equiv R_3$ is considered as a starting position for overtaking vehicle 2 (see Fig. 4), which is exactly the same scenario as in the on-vehicle overtaking described here.

Thus, the same procedure for deriving the kinematic model of vehicle 1 (29)–(31) can be applied for deriving the kinematic model of vehicle 2 with respect to points $R_4$, $R_5$, and $R_6$, respectively, as well the same relationships for the intervehicle kinematics (40) hold.

## III. Problem Formulation

In this paper, we consider autonomous overtaking maneuver without any information obtained from road infrastructure or communicated from the overtaken vehicle. The only information that the overtaking (automatic) vehicle can use for feedback control is the current relative position and orientation with respect to the overtaken vehicle given by (36), which are assumed to be available from onboard sensors.

### A. Trajectory Planning

For brevity, in the exposition which follows, we will derive in detail the trajectory planning procedure with respect to the first phase of the overtaking maneuver. Similar relationships can be also derived for Phase 2 and Phase 3. Index 1 will be also omitted and we will denote the pose error $e_1 = [e_{x1} \quad e_{y1} \quad e_{\theta 1}]^T$ by $e = [e_x \quad e_y \quad e_\theta]^T$. We consider in detail the problem of generating smooth trajectories for point to point motion in terms of the posture errors $(e_x, e_y)$ with respect to the moving reference frame $R_1 x_{R1} y_{R1}$, which is rigidly linked to the overtaken vehicle. Assuming rectilinear motion of the overtaken vehicle, we are interested in the overtaking scenario for the first phase when the overtaking vehicle starts the maneuver from an initial position and orientation behind the overtaken vehicle with a given velocity. At the end of the first phase, the two vehicles have to be (almost) parallel and at the same time, the desired position of the overtaking vehicle behind the overtaken vehicle has to be shifted at distances $L_{t1}$ and $L_{n1}$ in longitudinal and lateral direction, respectively (see Fig. 3). These distances are determined from considerations of safety driving and sensor requirements (in particular, $L_{t1}$ may be equal to zero). In addition, the relative intervehicle velocity in longitudinal direction must be equal to a prescribed nonzero value. For this end, we suppose that at time $t_0$, the state variables satisfy

$$\begin{matrix} e_x^d(t_0) = e_{x0} \\ \dot{e}_x^d(t_0) = \dot{e}_{x0} \end{matrix}; \quad \begin{matrix} e_y^d(t_0) = e_{y0} \\ \dot{e}_y^d(t_0) = \dot{e}_{y0} \end{matrix}. \tag{41}$$

At time $t_f$, we wish to attain the values

$$\begin{matrix} e_x^d(t_f) = 0 \\ \dot{e}_x^d(t_f) = \Delta v_{Rx}(t_f) \end{matrix}; \quad \begin{matrix} e_y^d(t_f) = 0 \\ \dot{e}_y^d(t_f) = 0 \end{matrix} \tag{42}$$

where $\Delta v_{Rx}(t_f)$ is the prescribed relative nonzero intervehicle velocity in $x_{R1}$-direction at $t_f$, i.e., the overtaking vehicle has to start the second phase of the overtaking maneuver at prescribed velocity, which is higher compared with the velocity of the overtaken vehicle. The magnitude of this relative

intervehicle velocity is set as some part of the velocity estimate of the overtaken vehicle in the beginning $(t_0)$ of each phase. A specific feature of the trajectory planning procedure is that the initial values of the program errors $(e_x^d(t_0), e_y^d(t_0))$ are equal to the current values $(e_x(t_0), e_y(t_0))$ at $t = t_0$, and in such a way, a smooth transition between the adjacent phases is assured. From a practical point of view, the following conditions have to be satisfied: $e_x(t_0) \in [a_x, b_x]$ where $a_x < b_x$, and $e_y(t_0) \in [a_y, b_y]$ where $a_y < b_y$. The constants $a_x$, $b_x$, $a_y$, and $b_y$ are determined from considerations of safety driving, sensor requirements, and the vehicle's geometrical (for example, limitations for the front-wheel steering angle) and dynamical limitations (lateral acceleration limits), as well as power and acceleration capabilities. In this paper, we consider cubic polynomials for the desired trajectories of the form

$$\begin{aligned} e_x^d(t) &= a_{0x} + a_{1x}(t-t_0) + a_{2x}(t-t_0)^2 + a_{3x}(t-t_0)^3 \\ e_y^d(t) &= a_{0y} + a_{1y}(t-t_0) + a_{2y}(t-t_0)^2 + a_{3y}(t-t_0)^3. \end{aligned} \tag{43}$$

Differentiating (43) with respect to time, we obtain quadratic polynomials with respect to the derivatives $\dot{e}_x^d(t)$ and $\dot{e}_y^d(t)$, i.e.,

$$\begin{aligned} \dot{e}_x^d(t) &= a_{1x} + 2a_{2x}(t-t_0) + 3a_{3x}(t-t_0)^2 \\ \dot{e}_y^d(t) &= a_{1y} + 2a_{2y}(t-t_0) + 3a_{3y}(t-t_0)^2. \end{aligned} \tag{44}$$

Using (41)–(44), we obtain eight equations for the eight unknown coefficients $a_{1x}$, $a_{2x}$, $a_{3x}$, $a_{4x}$ and $a_{1y}$, $a_{2y}$, $a_{3y}$, and $a_{4y}$. Time $t_f$ determines the duration of Phase 1. Since in this paper, the desired trajectories (43), together with the derived kinematic relationships between the vehicles, are used to establish a foundation for designing kinematics-based feedback control, we assume that these trajectories have been tailored in accordance with the feasibility requirements, as maximum longitudinal acceleration, maximum lateral acceleration, and maximum speed.

Similar expressions for the desired trajectories can be assigned for Phase 2 and Phase 3.

### B. Problem Statement

We assume that we are able to measure the pose error $e = [e_x \quad e_y \quad e_\theta]^T \in \Re^3$ defined in (36), but the linear velocity $v_{1x}$ of the overtaken vehicle is an unknown parameter.

Given the intervehicle kinematics in error coordinates (40), the control objective for Phase 1 is to asymptotically regulate to zero the coordinates $(e_x, e_y)$ of the reference point $L$ of the overtaking vehicle with respect to the coordinate frame $R_1$ (attached to the overtaken vehicle) in accordance with the desired trajectories (43) with respect to the error coordinates $(e_x, e_y)$ with initial and final conditions given by (41) and (42). Similar objectives can be formulated for Phase 2 and Phase 3, where the virtual reference points associated with the overtaken vehicle are $R_2$ and $R_3$, respectively.

## IV. Adaptive Control Design

### A. Overtaken Vehicle With Constant Velocity

We deal with the problem of controlling the motion of the overtaking vehicle during the overtaking maneuver, when the overtaken vehicle moves straight with constant velocity. Phase 1 of the overtaking maneuver once again is considered in detail. We make the following change of coordinates:

$$\begin{aligned} x_e &= e_x - e_x^d \\ y_e &= e_y - e_y^d \end{aligned} \tag{45}$$

where the pose error coordinates $(e_x, e_y)$ are defined by (37), and the desired trajectories $(e_x^d(t), e_y^d(t))$ are given by (43).

The model (40) describing intervehicle kinematics in error coordinates is redefined in terms of the new coordinates (45) as follows:

$$\begin{aligned} \dot{x}_e &= u_1 - v_{1x} - \dot{e}_x^d \\ \dot{y}_e &= u_2 - \dot{e}_y^d \\ \dot{e}_\theta &= -\frac{\sin e_\theta}{L_2} u_1 + \frac{\cos e_\theta}{L_2} u_2. \end{aligned} \tag{46}$$

The adaptive control design is based on a reduced-order system composed of the first two equations of (46) rewritten below for clarity of exposition, i.e.,

$$\begin{aligned} \dot{x}_e &= u_1 - v_{1x} - \dot{e}_x^d \\ \dot{y}_e &= u_2 - \dot{e}_y^d. \end{aligned} \tag{47}$$

Consider system (47) and assume that the velocity of the overtaken vehicle $v_{1x} = cte > 0$ is unknown constant parameter. The control problem consists in finding an adaptive feedback control law for system (47) with inputs $(u_1, u_2)$ such that

$$\lim_{t\to\infty}(x_e(t)) = 0 \quad \text{and} \quad \lim_{t\to\infty}(y_e(t)) = 0. \tag{48}$$

Consider the control

$$\begin{aligned} u_1 &= \hat{v}_{1x} + \dot{e}_x^d - k_x x_e \\ u_2 &= \dot{e}_y^d - k_y y_e \end{aligned} \tag{49}$$

where $k_x$ and $k_y$ are positive gains, and $\hat{v}_{1x}$ is the estimate of the overtaken vehicle velocity. We chose the following Lyapunov function candidate:

$$V = \frac{1}{2}x_e^2 + \frac{1}{2}y_e^2 + \frac{1}{2\gamma_v}\widetilde{v}_{1x}^2 \tag{50}$$

where

$$\widetilde{v}_{1x} = \hat{v}_{1x} - v_{1x} \tag{51}$$

is the parameter error, and $\gamma_v = cte > 0$ is the adaptation gain. Using (47), (49), and (51), the derivative of $V$ is obtained in the form

$$\dot{V} = -k_x\dot{x}_e^2 - k_y\dot{y}_e^2 + \widetilde{v}_{1x}\left(x_e + \frac{1}{\gamma_v}\dot{\hat{v}}_{1x}\right). \tag{52}$$

Choosing the update law as

$$\dot{\hat{v}}_{1x} = -\gamma_v x_e \tag{53}$$

we get for the derivative of $V$, i.e.,

$$\dot{V} = -k_x \dot{x}_e^2 - k_y \dot{y}_e^2 \leq 0. \tag{54}$$

The resulting closed-loop adaptive system becomes

$$\begin{aligned} \dot{x}_e &= -k_x x_e + \widetilde{v}_{1x} \\ \dot{y}_e &= -k_y y_e \\ \dot{\widetilde{v}}_{1x} &= -\gamma_v x_e. \end{aligned} \tag{55}$$

*Proposition 1:* Assume that the linear velocity of the overtaken vehicle is a bounded unknown constant parameter $v_{1x} = cte > 0$ and also that $L_2 \neq 0$. If the control law given by (49) is applied to (47), where the velocity estimate $\hat{v}_{1x}$ is obtained from the parameter update law (53), the origin $o_Z = [x_e, y_e, \widetilde{v}_{1x}]^T = 0$ of the closed-loop system (55) is asymptotically stable.

*Proof:* System (55) has an equilibrium point at the origin. Function (50) is continuously differentiable and positive definite, and its derivative (54) along the trajectories of the system is negative semidefinite. From (54), it follows that (50) is nonincreasing, $(V(t) \leq V(0))$, and this, in turn, implies that $x_e(t)$, $y_e(t)$, and $\widetilde{v}_{1x}(t)$ are uniformly bounded with respect to the initial conditions.

To characterize the set $S = \{o_Z \in \Re^3 | \dot{V}(z) = 0\}$, note that

$$\dot{V}(z) = 0 \Rightarrow x_e = 0 \quad \text{and} \quad y_e = 0. \tag{56}$$

Hence, $S = \{o_Z \in \Re^3 | x_e = 0; y_e = 0\}$. To prove asymptotic stability of the equilibrium point $o_Z = 0$, we use the LaSalle invariance principle [38]. Suppose that $o_Z(t)$ is a trajectory that identically belongs to $S$. From (54), we have

$$\begin{aligned} &x_e(t) \equiv 0 \Rightarrow \dot{x}_e \equiv 0 \Rightarrow \widetilde{v}_{1x} \equiv 0 \\ &y_e(t) \equiv 0 \Rightarrow \dot{y}_e \equiv 0 \\ &x_e(t) \equiv 0 \Rightarrow \dot{\widetilde{v}}_{1x} \equiv 0. \end{aligned} \tag{57}$$

Therefore, the only solution that can stay in $S$ is the trivial solution $o_z(t) = 0$, and the origin is asymptotically stable.

Since the dynamics of $e_\theta$ was not taken into account in the feedback control design, the next step in the stability analysis is to establish that $e_\theta$ is bounded in the interval $[t_0, t_f]$. From (46), using the control (49), the third equation for $e_\theta$ takes the form of a perturbed system

$$\dot{e}_\theta = f(e_\theta) + g(t, e_\theta) \tag{58}$$

where the nominal system is given by

$$\dot{e}_\theta = f(e_\theta) = -\frac{v_{1x}}{L_2} \sin e_\theta \tag{59}$$

and the perturbation term is obtained in the form

$$\begin{aligned} g(t, e_\theta) = \frac{1}{L_2} [&-(\widetilde{v}_{1x} - k_x x_e) \sin e_\theta - k_y y_e \cos e_\theta \\ &- \dot{e}_x^d \sin e_\theta + \dot{e}_y^d \cos e_\theta]. \end{aligned} \tag{60}$$

Since $x_e(t)$, $y_e(t)$, and $\widetilde{v}_{1x}(t)$ are uniformly bounded, ($\sin(e_\theta)$ and $\cos(e_\theta)$ are bounded functions), and the polynomial functions (44) are bounded within the interval $[t_0, t_f]$, it follows that:

$$\|g(t, e_\theta)\| \leq \lambda \tag{61}$$

in the domain of interest, $\lambda$ is a positive constant. Point $e_\theta = 0$ is an exponentially stable equilibrium point for the nominal system (59), which can be easily proved by using, for example, the Lyapunov function $W = 1 - \cos e_\theta$. Therefore, $e_\theta$ is bounded and $e_\theta(t) \to 0$ as $t \to \infty$. If $e_{\theta n}(t)$ and $e_{\theta p}(t)$ are the solutions of the nominal and perturbed systems (59) and (58), respectively, using the Gronwall–Bellman inequality [38], we have on the compact time interval $[t_0, t_f]$, i.e.,

$$\begin{aligned} \|e_{\theta n}(t) - e_{\theta p}(t)\| \leq \|e_{\theta n}(t_0) - e_{\theta 0}(t)\| \exp[l(t - t_0)] \\ + \frac{\lambda}{l} \{\exp[l(t - t_0)] - 1\} \end{aligned} \tag{62}$$

where $l$ is a Lipschitz constant for the nominal system (59). Hence, $e_{\theta p}(t)$ is bounded on the time interval $[t_0, t_f]$.

### B. Overtaken Vehicle With Time-Varying Velocity

In Proposition 1, asymptotic stability of the equilibrium point $o_Z = [x_e, y_e, \widetilde{v}_{1x}]^T = 0$ of the closed-loop system (55) is claimed when the linear velocity of the overtaken vehicle is unknown but constant parameter. In case of time-varying bounded velocity $v_{1x}(t)$, when the update law is of form (53), the resulting closed-loop adaptive system becomes

$$\dot{o}_Z = A o_z + \xi(t) \tag{63}$$

where

$$o_Z = [x_e, y_e, \widetilde{v}_{1x}]^T \in \Re^3 \tag{64}$$

$$A = \begin{bmatrix} -k_x & 0 & 1 \\ 0 & -k_y & 0 \\ -\gamma_v & 0 & 0 \end{bmatrix} \in \Re^{3\times 3} \tag{65}$$

$$\xi = [\,0 \quad 0 \quad -\dot{v}_{1x}\,]^T \in \Re^3 \tag{66}$$

and $\dot{v}_{1x}$ is the longitudinal acceleration of the overtaken vehicle. System (63) can be viewed as a perturbation of a nominal stable linear time-invariant system (55) where the perturbation is a uniformly bounded function of time that satisfies

$$|\dot{v}_{1x}(t)| \leq a \tag{67}$$

for all $t \geq 0$. In this case, we cannot study stability of the $o_Z = 0$ as an equilibrium point, and we analyze under which conditions the solution $o_Z(t)$ of the perturbed system (63) will be ultimately bounded. Notice that asymptotic stability of (55), as discussed in Proposition 1, Section III, implies exponential stability due to a closed-loop system linearity [38]. Since $A$ is a Hurwitz matrix, there is a unique solution $P = P^T > 0$ of the Lyapunov equation

$$PA + A^T P = -Q \tag{68}$$

for given $Q = Q^T > 0$. We form a quadratic Lyapunov function $V(o_Z)$ in the form

$$V(o_z) = o_Z^T P o_z. \tag{69}$$

Function (61) satisfies the inequalities

$$\rho_{\min}(P)\|o_Z\|^2 \le V(o_Z) \le \rho_{\max}(P)\|o_Z\|^2 \tag{70}$$

$$\dot{V} = \frac{\partial V}{\partial o_Z} A o_Z \le -\rho_{\min}(Q)\|o_Z\|^2 \tag{71}$$

$$\left\| \frac{\partial V}{\partial o_Z} \right\| \le 2\rho_{\max}(P)\|o_Z\| \tag{72}$$

where $\rho_{min}(P)$, $\rho_{max}(P)$, and $\rho_{min}(Q)$, $\rho_{max}(Q)$ denote the smallest and the largest eigenvalues of $P$ and $Q$, respectively.

Suppose that the perturbation $\xi$ satisfies the inequality

$$\|\xi\| \le a < \frac{\rho_{\min}(Q)}{2\rho_{\max}(P)} \sqrt{\frac{\rho_{\min}(P)}{\rho_{\max}(P)}} \varphi s \tag{73}$$

for all $t \ge 0$, for $S_0 = \{o_Z \in \Re^3 | \|o_Z\| < s\}$, and some positive constant $\varphi$. Using (70)–(72), for the derivative of $V$ along the trajectories of the perturbed system (63), we have

$$\begin{aligned} \dot{V} &= \frac{\partial V}{\partial o_Z}(A o_Z + \xi) = -o_Z^T Q o_Z + 2 o_Z^T P \xi \\ &\le -\rho_{\min}(Q)\|o_Z\|^2 + 2\left\| o_Z^T \rho_{\max}(P)\xi \right\| \\ &\le -\rho_{\min}(Q)\|o_Z\|^2 + 2\rho_{\max}(P) a \|o_Z\| \\ &\le -(1-\varphi)\rho_{\min}(Q)\|o_Z\|^2 \end{aligned} \tag{74}$$

for $0 < \varphi < 1$ and for $\|o_Z\| > (2a\rho_{\max}(P)/\varphi\rho_{\min}(Q))$. Based on Lemma 5.2 and Corollary 5.3 [37], it follows that for all $\|o_Z(t_0)\| < \sqrt{(\rho_{\min}(P)/\rho_{\max}(P))}s$, the solution $o_Z(t)$ of system (63) satisfies

$$\|o_Z(t)\| \le c\|o_Z(t_0)\| \exp\left[-m(t-t_0)\right], \quad t_0 \le t < t_1 \tag{75}$$

for some finite $t_1$, and

$$\|o_Z(t)\| \le \mu, \quad t \ge t_1 \tag{76}$$

where

$$c = \frac{\rho_{\max}(P)}{\rho_{\min}(P)}, \quad m = \frac{(1-\varphi)\rho_{\min}(Q)}{2\rho_{\max}(P)}$$

$$\mu = \frac{2\rho_{\max}(P)}{\rho_{\min}(Q)} \sqrt{\frac{\rho_{\max}(P)}{\rho_{\min}(P)}} \frac{a}{\varphi}. \tag{77}$$

The designed control law (49)–(53) constitutes the upper level controller of the overtaking vehicle and provides reference signals to the lower level controller for the steering and velocity dynamics, which have to be tracked. The same approach can be used to derive feedback controllers for the overtaking vehicle for Phase 2 and Phase 3.

TABLE I
COORDINATES OF THE REFERENCE FRAMES IN THE OVERTAKEN VEHICLE FRAME

| Phase | Reference Frame | Coordinates |
|---|---|---|
| 1 | $R_1x_{R1}y_{R1}$ | $L_{t1}$ = -1m; $L_{n1}$ = 3m |
| 2 | $R_2x_{R2}y_{R2}$ | $L_{t2}$ = 8m; $L_{n2}$ = 3m |
| 3 | $R_3x_{R3}y_{R3}$ | $L_{t3}$ = 12m; $L_{n3}$ = 0m |

*Remark 3:* The control law (49), together with the adaptive update law (53), has been synthesized under the assumption of no communication between the vehicles. It should be noticed that, in the case of intervehicle communication, the same structure of the control law (49) and the same reference trajectories (43) can be used with the only difference that in (49), the estimate of the overtaken vehicle velocity $\hat{v}_{1x}$ obtained from (53) has to be replaced by its real value. In addition, if information obtained from DGPS is available, the pose error defined in (36) can be determined from (37).

## V. SIMULATION RESULTS

To illustrate the effectiveness of the proposed controller, several simulations are carried out in order to evaluate the intervehicle behavior and tracking accuracy during the three-phase overtaking maneuver. In the simulation using MATLAB, a planar bicycle 2DOFs vehicle model is used. The coordinates of the reference frames $R_1x_{R1}y_{R1}$, $R_2x_{R2}y_{R2}$, and $R_3x_{R3}y_{R3}$ with respect to the coordinate frame $P_1x_{P1}y_{P1}$ (see Fig. 3), attached to the midpoint of the rear vehicle axle of the overtaken vehicle for every phase of the three-phase overtaking maneuver is provided in Table I.

The longitudinal vehicle base of the overtaking vehicle was chosen to be $l_2 = 2$ m. The initial position and orientation of the overtaking vehicle in the inertial frame $Fxy$ are ${}^F x_{P2}(0) =$ 0 m; ${}^F y_{P2}(0) = 0$ m; and $\theta_2(0) = 0$ rad. The initial position and orientation of the overtaken vehicle in $Fxy$ are ${}^F x_{P1}(0) =$ 8 m; ${}^F y_{P1}(0) = 0$ m; and $\theta_1(0) = 0$ rad. The desired intervehicle distance in the beginning of the maneuver is set to be 6 m. The duration of every phase of the maneuver was chosen to be $t_{int} = 5$ s.

For the first set of simulations, the velocity of the overtaken vehicle was piecewise constant and was set to be equal to 10, 15, and 10 m/s for Phase 1, Phase 2, and Phase 3, respectively. The overtaking vehicle was initially traveling at a velocity of 10 m/s. Figs. 5–8 are the corresponding plots when the velocity of the overtaken vehicle is piecewise constant.

From Fig. 5, we can see the planar path in the $x-y$ plane, drown by the vehicle guide points $P_1$ (dashed line) and $P_2$ (solid line) of the overtaken and overtaking vehicle, respectively. The path profile of the overtaking vehicle shows that during the second phase, the vehicles were traveling parallel paths with a prescribed intervehicle distance of 3 m, which is equal to $L_{n1} = L_{n2}$ (see Table I).

In Fig. 6, the evolution in time of velocities of the overtaking vehicle $v_{2x}(t)$ (solid line), the overtaken vehicle $v_{1x}(t)$ (dashed line), and the estimate $\hat{v}_{1x}(t)$ of the overtaken vehicle velocity

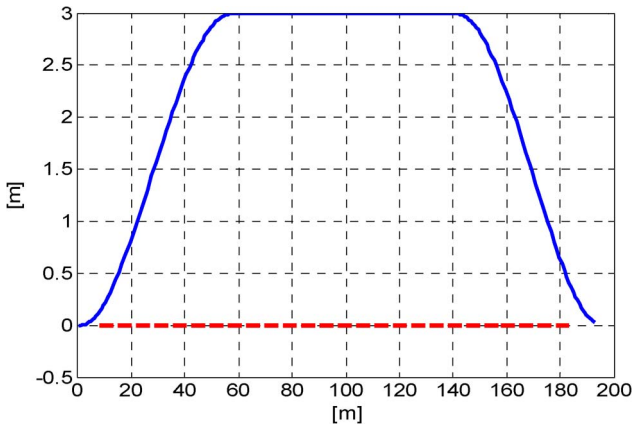


Fig. 5. Planar path drown by the vehicle guide points (the midpoints of the rear vehicle axles): (solid line) overtaking vehicle and (dashed line) overtaken vehicle.

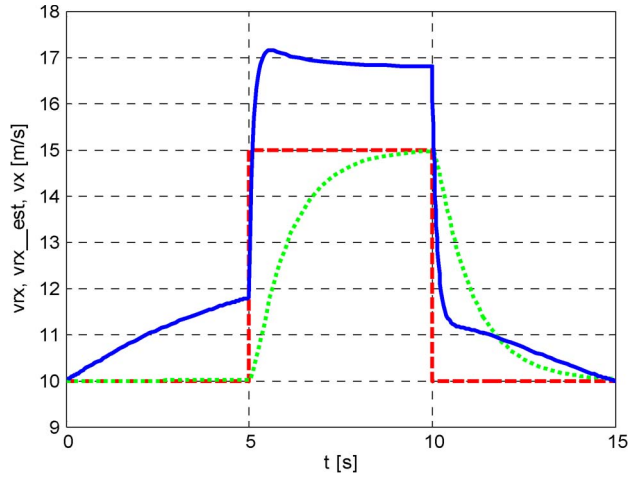


Fig. 6. Time history of the actual vehicle velocities: (solid line) overtaking vehicle, (dashed line) overtaken vehicle, and (dotted line) the estimate of the overtaken vehicle velocity.

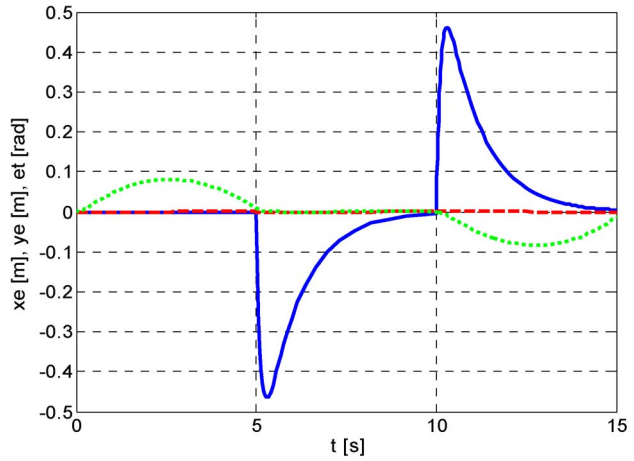


Fig. 7. Time history of the error coordinates.

(dotted line) obtained from the adaptive update law is shown. The estimate of the overtaken vehicle velocity asymptotically tends to its actual value. At the end of the third phase of the overtaking maneuver, the overtaking vehicle attains a prescribed velocity (in this simulation, this velocity was chosen to be equal to the overtaken vehicle, and the two vehicles are traveling at a same velocity).

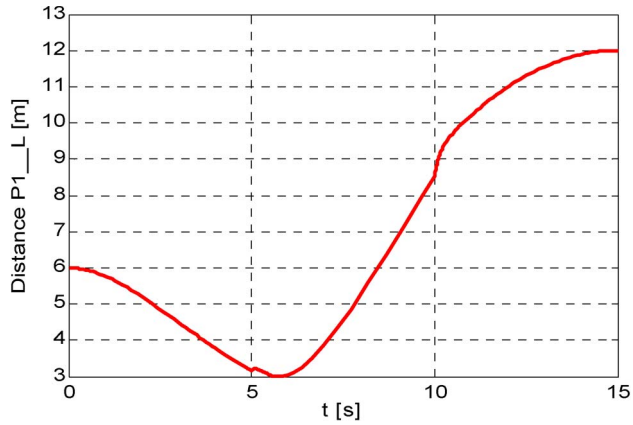


Fig. 8. Time history of the intervehicle distance.

In Fig. 7, the evolution in time of the error coordinates $x_e(t)$ (solid line), $y_e(t)$ (dashed line), and the orientation error between the two vehicles $e_\theta(t)$ (dotted line) is shown. The error coordinates asymptotically tend to zero. The larger longitudinal error $x_e(t)$ in the beginning of the second and the third phase (about 0.45 m) is due to the jump in the velocity of the overtaken vehicle (from 10 to 15 m/s and again from 15 to 10 m/s), and some time needed for obtaining estimates for these velocities. The performance of the adaptive controller depends on the adaptation gain $\gamma_v$. A small gain will lead to slow adaptation, and the transient tracking error will be large. However, too large gain will lead to oscillatory transient.

The evolution in time of the intervehicle distance $P_1L$ (see Fig. 3) is given in Fig. 8. This quantity may be considered as a "separation distance" between the two vehicles. The smallest value (3 m) was obtained in the beginning of the second phase [just after traveling the distance $L_{t1}$ (see Fig. 3)], when the front bumper of the overtaken vehicle is aligned with the rear bumper of the overtaken vehicle, and this is exactly the distance $L_{n1} = 3$ m given in Table I. At the end of the third phase of the overtaking maneuver, distance $P_1L$ becomes equal to $L_{t3} = 12$ m (see Table I), which is another illustration that the position of point $L$ of the overtaking vehicle coincides at this time instant with the virtual reference point $R3$ attached to the overtaken vehicle (see Fig. 3).

For the second set of simulations, the velocity of the overtaken vehicle was time varying, with a ramp profile during Phase 1 (starting from 10 until 2.5 m/s at the end of Phase 1, with constant deceleration of $-1.5$ m/s$^2$) and Phase 2 (starting from 2.5 until 10 m/s at the end of Phase 2, with constant acceleration of 1.5 m/s$^2$). For Phase 3, the velocity was chosen to be constant and equal to 10 m/s. Figs. 9–12 are the corresponding plots when the velocity of the overtaken vehicle is piecewise constant.

The planar path in the $x-y$ plane, drown by the vehicle guide points $P_2$ (solid line) and $P_1$ (dashed line) of the overtaken and overtaking vehicle, respectively, is shown in Fig. 9. Similarly to the first set of simulations with piecewise constant velocities for every interval, the path profile of the overtaking vehicle

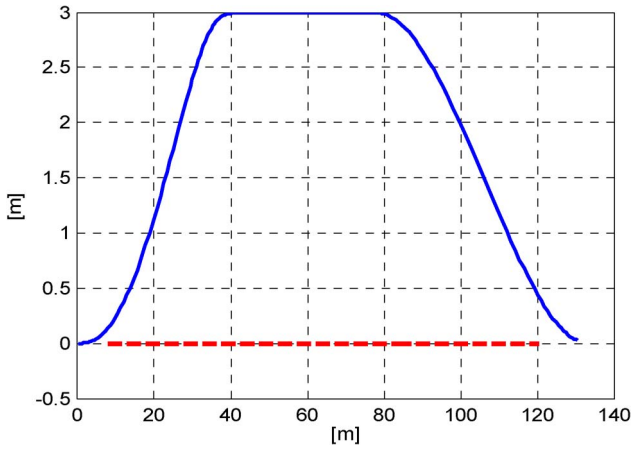


Fig. 9. Planar path drown by the vehicle guide points (the midpoints of the rear vehicle axles): (solid line) overtaking vehicle and (dashed line) overtaken vehicle.

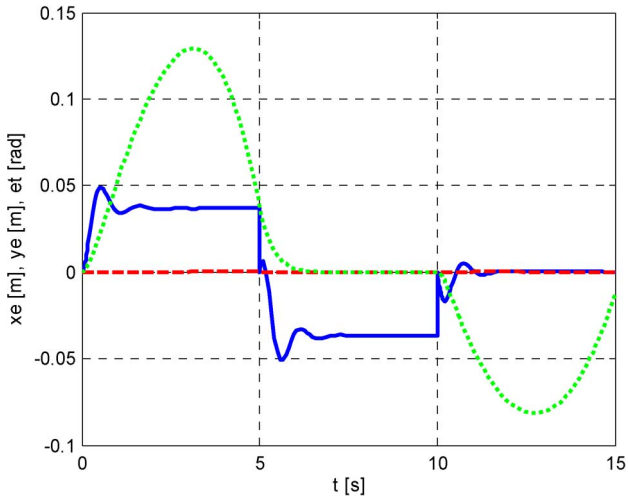


Fig. 11. Time history of the error coordinates.

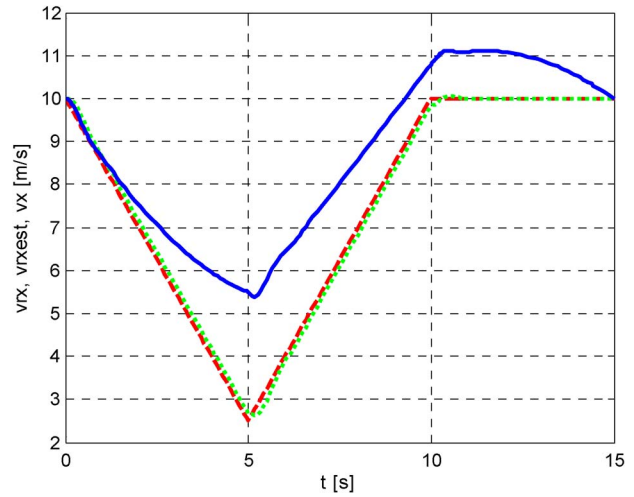


Fig. 10. Time history of the actual vehicle velocities: (solid line) overtaking vehicle, (dashed line) overtaken vehicle, and (dotted line) the estimate of the overtaken vehicle velocity.

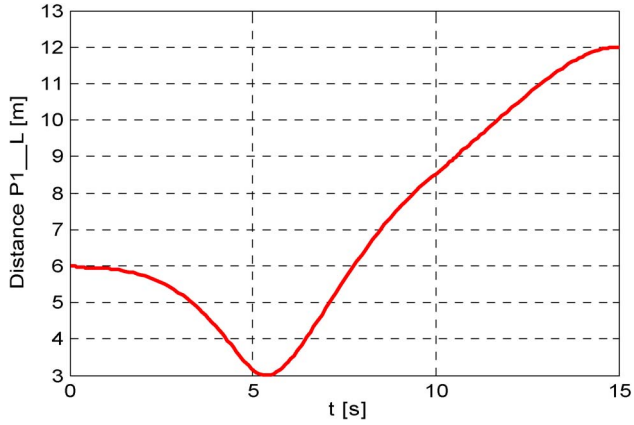


Fig. 12. Time history of the intervehicle distance.

shows that during the second phase, the vehicles were traveling parallel paths with a prescribed intervehicle distance of 3 m, which is equal to $L_{n1} = L_{n2}$ (see Table I).

In Fig. 10, the evolution in time of velocities of the overtaking vehicle $v_{2x}(t)$ (solid line), the overtaken vehicle $v_{1x}(t)$ (dashed line), and the estimate $\hat{v}_{1x}(t)$ of the overtaken vehicle velocity (dotted line) obtained from the adaptive update law is shown. The estimate of the overtaken vehicle velocity is closed to the actual velocity of the overtaken vehicle during Phase 1 and Phase 2 when the velocity of the overtaken vehicle is not constant. In the third phase of the overtaking maneuver, the velocity estimate asymptotically tends to its actual value, since the velocity of the overtaken vehicle is constant.

Fig. 11 shows the evolution in time of the error coordinates $x_e(t)$ (solid line), $y_e(t)$ (dashed line), and the orientation error $e_\theta(t)$ between the two vehicles (dotted line).

With conformity with the analytical result obtained in Section IV-B for the stability properties of the adaptive closed-loop system in the case of the time-varying velocity of the overtaken vehicle, the error coordinates $x_e(t)$, $y_e(t)$ are bounded during Phase 1 and Phase 2 when the velocity of the overtaken vehicle is not constant. In the third phase of the overtaking maneuver, these errors asymptotically tend to zero, since the velocity of the overtaken vehicle is constant.

The evolution in time of the intervehicle distance $P_1L$ (see Fig. 3) is given in Fig. 12. The profile is similar to those shown in Fig. 8. Again, the smallest value (3 m) was obtained in the beginning of the second phase, when the front bumper of the overtaken vehicle is aligned with the rear bumper of the overtaken vehicle.

The results of the simulation confirm the stability properties of the proposed controller.

## VI. Conclusion

In this paper, a nonlinear adaptive controller for two-vehicle automated overtaking maneuvers has been presented. We consider the problem of a three-phase overtaking without the use of information obtained from road infrastructure or intervehicle communication. Applying standard robotic nomenclature for translational and rotational displacements and velocities, a methodology for kinematic modeling of the vehicles during

the overtaking maneuver has been developed, and relative intervehicle kinematics has been formulated. The proposed methodology for modeling one-vehicle overtaking by using reference way points can be extended to multivehicle overtaking. Continuous reference trajectories for every phase using third-order polynomial interpolation method have been generated in real time and consecutively tracked. The reference trajectories, together with the derived kinematic relationships between the vehicles, have been used to establish a foundation for designing kinematics-based feedback control. The designed feedback controller requires information only for the current relative intervehicle position and orientation. The unknown velocity of the overtaken vehicle has been estimated using adaptive update law. The stability of the closed-loop system was analytically studied, and the asymptotic stability of the closed-loop control system was proven in case of constant velocity of the overtaken vehicle. In addition, in case of time-varying, but bounded velocity, ultimate boundness of the system tracking error was claimed. Simulation results have been presented in order to illustrate the stability properties and performance of the proposed controller. An autonomous overtaking control system may constitute a backup system for the infrastructure-based control system when the letter is malfunctioning or due to the failure the intervehicle communication.

## REFERENCES


[1] S. Shladover, "The GM-PATH platoon scenario," *Intellimotion*, vol. 6, no. 3, pp. 2–3, 1997.

[2] R. Kianfar, B. Augusto, A. Ebadighajari, U. Hakeem, J. Nilsson, A. Raza, R. Tabar, N. Irukulapati, C. Englund, P. Falcone, S. Papanastasiou, L. Svensson, and H. Wymeersch, "Design and experimental validation of a cooperative driving system in the grand cooperative driving challenge," *IEEE Trans. Intell. Transp. Syst.*, vol. 13, no. 3, pp. 994–1007, Sep. 2012.

[3] E. van Nunen, M. Kwakkernaat, J. Ploeg, and B. Netten, "Cooperative competition for future mobility," *IEEE Trans. Intell. Transp. Syst.*, vol. 13, no. 3, pp. 1018–1025, Sep. 2012.

[4] K. Lindsrom, K. Sjoberg, U. Holmberg, J. Anderson, F. Bergh, M. Bjade, and S. Mak, "A modular CACC system integration and design," *IEEE Trans. Intell. Transp. Syst.*, vol. 13, no. 3, pp. 1050–1061, Sep. 2012.

[5] L. Guvenc, I. Uygan, K. Kahraman, R. Karaahmetoglu, I. Altay, M. Senturk, M. Emirler, A. Karci, B. Guvenc, E. Altug, M. Turan, O. Tas, E. Bozkurt, U. Ozgunter, K. Redmill, A. Kurt, and B. Efendioglu, "Cooperative adaptive cruise control implementation of team Mekar at the grand cooperative driving challenge," *IEEE Trans. Intell. Transp. Syst.*, vol. 13, no. 3, pp. 1062–1074, Sep. 2012.

[6] M. Nieuwenhuijze, T. van Keulen, S. Oncu, B. Bonsen, and H. Nijmeijer, "Cooperative driving with a heavy-duty truck in mixed traffic: Experimental results," *IEEE Trans. Intell. Transp. Syst.*, vol. 13, no. 3, pp. 1026–1032, Sep. 2012.

[7] T. Fraichard, "CyberCar: L'alternative a la voiture particuliere," *Navigation*, vol. 53, no. 209, pp. 53–75, 2009.

[8] S. Hima, S. Glaser, A. Chaibet, and B. Vanholme, "Controller design for trajectory tracking of autonomous passenger vehicles," in *Proc. IEEE Conf. Intell. Transp. Syst.*, 2011, pp. 1459–1464.

[9] J. Alonso, E. Vidal, A. Rotter, and M. Muhlenberg, "Lane-change decision aid system based on motion-driven vehicle tracking," *IEEE Trans. Veh. Technol.*, vol. 57, no. 5, pp. 2736–2746, Sep. 2008.

[10] S. Sheikholeslam and A. Desoer, "Longitudinal control of a platoon of vehicles with no communication of lead vehicle information: A system level study," *IEEE Trans. Veh. Technol.*, vol. 42, no. 4, pp. 546–554, Nov. 1993.

[11] R. White and M. Tomizuka, "Autonomous following lateral control of heavy vehicles using laser scanning radar," in *Proc. Amer. Control Conf.*, 2001, pp. 2333–2337.

[12] S. Seshagiri and H. Khalil, "Longitudinal adaptive control of a platoon of vehicles," in *Proc. Amer. Control Conf.*, 1999, pp. 3681–3685.

[13] H. M. Lim and J. Karl Hedrick, "Lateral and longitudinal vehicle control coupling for automated vehicle operation," in *Proc. Amer. Control Conf.*, San Diego, CA, USA, 1999, pp. 3676–3680.

[14] S. Wu, H. Chiang, J. Perng, T. Lee, and C. Chen, "The automated lane-keeping design for an intelligent vehicle," in *Proc. IEEE Int. Veh. Symp.*, 2005, pp. 508–513.

[15] M. Oya and Q. Wang, "Adaptive lane keeping controller for four-wheel-steering vehicles," in *Proc. IEEE Int. Conf. Control Autom.*, Guangzhou, China, 2007, pp. 1942–1947.

[16] A. Ferrara and C. Vecchio, "Cruise control with collision avoidance for cars via sliding modes," in *Proc. IEEE Int. Symp. Intell. Control Appl.*, Munich, Germany, 2006, pp. 2808–2813.

[17] Y. Yoshida, Q. Wang, M. Oya, and K. Okumura, "Adaptive longitudinal velocity and lane keeping control of four-wheel-steering vehicles," in *Proc. SICE Annu. Conf.*, Takamatsu, Japan, 2007, pp. 1305–1310.

[18] H. Pham, M. Tomizuka, and J. Karl Hedrick, "Integrated maneuvering control for automated highway systems based on a magnetic reference/sensing system," Univ. California Berkeley, Berkeley, CA, USA, California PATH Res. Rep., UCB-ITS-PRR-97-28, 1997.

[19] T. Hessburg and M. Tomizuka, "Fuzzy logic control for lane change maneuvers in lateral vehicle guidance," Univ. California Berkeley, Berkeley, CA, USA, UCB-ITS-PWP-95-13, 1995.

[20] W. Chee and M. Tomizuka, "Vehicle lane change maneuver in automated highway systems," Univ. California Berkeley, Berkeley, CA, USA, California PATH Res. Rep., UCB-ITS-PRR-94-92, 1994.

[21] T. Lee, B. Kim, K. Yi, and C. Jeong, "Development of lane change driver model for closed-loop simulation of the active safety system," in *Proc. IEEE Conf. Intell. Transp. Syst.*, 2011, pp. 56–61.

[22] A. Piazzi and C. Bianco, "Quantic G2-splines for trajectory planning of autonomous vehicles," in *Proc. IEEE Int. Veh. Symp.*, 2000, pp. 198–203.

[23] I. Papadimitriou and M. Tomizuka, "Fast lane changing computations using polynomials," in *Proc. Amer. Control Conf.*, 2003, pp. 48–53.

[24] P. Resende and F. Nashashibi, "Real-time dynamic trajectory planning for highly automated driving in highways," in *Proc. IEEE Conf. Intell. Transp. Syst.*, 2010, pp. 653–658.

[25] W. Chee and M. Tomizuka, "Unified lateral motion Control of vehicles for lane change maneuvers in automated highway systems," Univ. California Berkeley, Berkeley, CA, USA, California PATH Res. Rep. UCB-ITS-PRR-97-29, 1997.

[26] C. Hatipoglu, Ü. Özgüner, and K. Redmill, "Automated lane change controller design," *IEEE Trans. Intell. Transp. Syst.*, vol. 4, no. 1, pp. 13–22, Mar. 2003.

[27] P. Petrov and F. Nashashibi, "Planning and nonlinear adaptive control for an automated overtaking maneuver," in *Proc. 14th Int. IEEE Conf. Intell. Transp. Syst.*, Washington, DC, USA, 2011, pp. 662–667.

[28] T. Shamir, "How should an autonomous vehicle overtake a slower moving vehicle: Design and analysis of an optimal trajectory," *IEEE Trans. Autom. Control*, vol. 49, no. 4, pp. 607–610, Apr. 2004.

[29] U. Ghumman, F. Kunwar, and B. Benhabib, "Guidance-based on-line motion planning for autonomous highway overtaking," *Int. J. Smart Sens. Intell. Syst.*, vol. 1, no. 2, pp. 549–571, Jun. 2008.

[30] R. Kala and K. Warwick, "Planning autonomous vehicles in the absence of speed lanes using lateral potentials," in *Proc. IEEE Intell. Veh. Symp.*, 2012, pp. 597–602.

[31] J. Naranjo, C. Gonzales, R. Garcia, and T. Pedro, "Lane-change fuzzy control in autonomous vehicles for the overtaking maneuver," *IEEE Trans. Intell. Transp. Syst.*, vol. 9, no. 3, pp. 438–450, Sep. 2008.

[32] F. Wang, M. Yang, and R. Yang, "Conflict-probability-estimation-based overtaking for intelligent vehicles," *IEEE Trans. Intell. Transp. Syst.*, vol. 10, no. 2, pp. 366–370, Jun. 2009.

[33] J. Baber, J. Kolodko, T. Noel, M. Parent, and L. Vlacic, "Cooperative autonomous driving: Intelligent vehicles sharing city roads," *IEEE Robot. Autom. Mag.*, vol. 12, no. 1, pp. 44–49, Mar. 2005.

[34] V. Milanes, D. Florca, J. Villagra, J. Perez, C. Fernandez, I. Parra, C. Gonzales, and M. Sotelo, "Intelligent automatic overtaking system using vision for vehicle detection," *Exp. Syst. Appl.*, vol. 39, no. 3, pp. 3362–3373, Feb. 2012.

[35] M. Spong and M. Vidyasagar, *Robot Dynamics and Control*. Hoboken, NJ, USA: Wiley, 1988.

[36] A. Lur'e, *Analytical Mechanics*. New York, NY, USA: Springer-Verlag, 2002.

[37] P. Petrov, "Robust trajectory tracking algorithms for a wheeled mobile robot," in *Proc. IEEE Ind. Electron., Control, Instrum.*, 1991, pp. 1071–1074.

[38] H. Khalil, *Nonlinear Systems,* 2nd ed. Englewood Cliffs, NJ, USA: Prentice-Hall, 1996.

**Plamen Petrov** received the B.Eng. and M.S. degrees in automatic control and applied mathematics in 1979 and 1982, respectively, and the Ph.D. degree in electrical engineering from the Technical University of Sofia, Sofia, Bulgaria, in 1993.

He was a Postdoctoral Fellow with the École Normale Supérieure de Cachan, Cachan, France, in 1993. He is currently an Associate Professor with the Faculty of Mechanical Engineering, Technical University of Sofia, where he gives courses in Automatic Control and Motion Control in Mechatronic Systems. He is the Head of the Laboratory of Mechatronic Systems with the Faculty of Mechanical Engineering. Since 2009, he has been also an Invited Professor with the Institut National de la Recherche en Informatique et Automatique (INRIA), Rocquencourt, France. His current research interests include nonlinear control, modeling and control of mobile robots and manipulators, automated vehicles, and vehicle platoons.

**Fawzi Nashashibi** (M'11) received the M.S. degree in automation, industrial engineering and signal processing and the Ph.D. degree in robotics from the Laboratory of Analysis and Architecture of Systems/Centre National de la Recherche Scientifique (LAAS/CNRS), Toulouse University, Toulouse, France, and the HDR Diploma (accreditation to research supervision) from Pierre and Marie Curie University (Paris 6), Paris, France.

Since November 2010, he has been the Senior Researcher and Program Manager of IMARA Team with the Institut National de la Recherche en Informatique et Automatique (INRIA), Rocquencourt, France. Since 1994, he has been the Senior Researcher and Program Manager with the Robotics Center, Ecole des Mines de Paris (Mines ParisTech), Paris and since May 2000, he has been an R&D Engineer and a Project Manager with Association pour la Recherche et le Developpment des Methodes et Processus Industriels, Paris. He was previously a Research Engineer with PROMIP, Toulouse, France (working on mobile robotics perception dedicated to space exploration) and a technical manager with Light Co., La Courneuve, France, where he led the developments of Virtal Reality/Augmented Reality applications. His main research topics are in environment perception and multisensor fusion, vehicle positioning and environment 3-D modeling with main applications in intelligent transport systems and robotics. He played key roles in more than 50 European and national French projects such as Carsense, ARCOS, ABV, LOVe, HAVE-it, SPEEDCAM, PICAV, CityMobil, . . ., some of which he is coordinating. He is also involved in many collaborations with French and international academics and industrial partners. He is the author of numerous publications and patents in the field of intelligent transportation systems and advanced driver assistance systems. His current interest focuses on advanced urban mobility through the design and development of highly automated transportation systems. This includes highly automated unmanned guided vehicles (such as Cybercars), as well as automated personal vehicles. Since 1994, he has been also a Lecturer in several universities (Mines ParisTech, Paris 8 Saint-Denis, Leonard de Vinci Univ.—ESILV professor, Telecom Sud Paris, INT Evry, Ecole Centrale d'Electronique, in the fields of image and signal processing, 3-D perception, 3-D info-graphics, mobile robotics, and C++/JAVA programming.

Dr. Nashashibi is a member of the IEEE Transactions on Intelligent Transportation Systems and the Robotics and Automation Societies. He is an Associate Editor of several IEEE international conferences such as International Conference on Robotics and Automation, International Conference on Intelligent Robots and Systems, and Intelligent Vehicles Symposium.